Article

Positive Feedback Regulation of Poly(ADP-ribose) Polymerase 1 and the DNA-PK Catalytic Subunit Affects the Sensitivity of Nasopharyngeal Carcinoma to Etoposide

Lingyu Zhang, Yingting Zhuang, Guihui Tu, Ding Li, Yingjuan Fan, Shengnan Ye, Jianhua Xu, Ming Zheng, Ying Wu,* and Lixian Wu*

Read Online

ACCESS | 📊 Metrics & More | 📖 Article Recommendations | 🆂🅸 Supporting Information

ABSTRACT: Etoposide (VP-16) is used for the treatment of various cancers, including nasopharyngeal carcinoma (NPC); however, cancers develop resistance to this agent by promoting DNA repair. The DNA-PK (DNA-PKcs) catalytic subunit and poly(ADP-ribose) polymerase 1 (PARP1) mediate acquired resistance and poor survival in NPC cells exposed to DNA damaging agents. DNA repair can alter the sensitivity of NPC cells to DNA damaging agents, and these two enzymes function concomitantly in response to DNA damage *in vivo*. Therefore, we explored the relationship between DNA-PKcs and PARP1, which may affect NPC cell survival by regulating DNA repair after VP-16 treatment. We performed quantitative real-time polymerase chain reaction, western blotting, and enzyme-linked immunoassays and found that DNA-PKcs knockdown downregulated the PARP1 and PAR expression. Conversely, PARP1 knockdown reduced DNA-PKcs activity, indicating the mutual regulation between DNA-PKcs and PARP1 in VP-16-induced DNA repair. Moreover, a combination treatment with olaparib (a PARP1 inhibitor) and NU7441 (a DNA-PKcs inhibitor) sensitized NPC cells to VP-16 *in vitro* and *in vivo*, suggesting that the combined treatment of olaparib, NU7441, and a DNA-damaging agent may be a successful treatment regimen in patients with NPC.
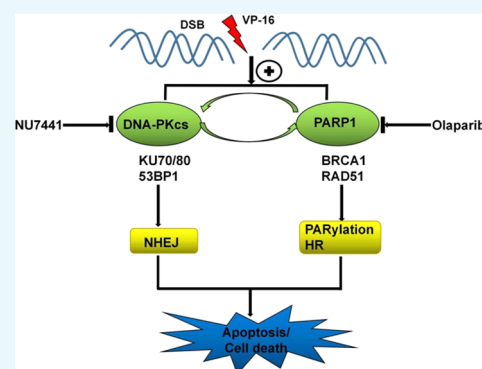
INTRODUCTION

Nasopharyngeal carcinoma (NPC), a common head and neck cancer in Southeast Asia and especially in southern China, is characterized by a high invasion rate and early metastasis.[1] Radiotherapy has been the primary treatment for NPC in general.[2] However, because >70% of newly diagnosed NPC cases present with locoregionally advanced disease,[2] concurrent chemoradiotherapy is now the standard treatment for the disease at this stage. Patients often initially respond to NPC treatment but later become resistant to these agents. Thus, effective therapeutic approaches for NPC are needed.[3]

Topoisomerase IIα (TopoIIα) has been reported to be overexpressed in a subset of NPCs, and TopoIIα upregulation is related to a worse prognosis and higher rates of local recurrence.[4] Biochemically, TopoIIα inhibition results in the stagnation of the replication fork and the eventual formation of a DNA double-strand break (DSB), which blocks the proliferation of cancer cells.[5] Etoposide (VP-16) is a TopoIIα inhibitor that has been clinically applied over the past decades and is a commonly prescribed anticancer drug worldwide.[5] However, VP-16 is generally administered at high doses to treat recurrent tumors, and the acute and cumulative toxicities of VP-16 to normal tissues limit its effectiveness.[6] Additionally, in recent years, the importance of DNA repair pathways in chemotherapy resistance has been increasingly recognized.[7] Pathways involved

in DNA repair include base excision repair (BER), homologous recombination (HR), mismatch repair (MMR), nucleotide excision repair (NER), nonhomologous end joining (NHEJ), and single-strand annealing (SSA).[8] Numerous studies have indicated that the HR and NHEJ pathways are responsible for the repair of TopoII-mediated DNA damage induced by VP-16.[9,10] Therefore, elucidating the molecular mechanisms of VP-16 resistance is of great importance for developing more efficient therapeutic strategies.

Poly(ADP-ribose) polymerase (PARP) binding to DNA damage sites increases its catalytic activity and triggers local poly(ADP-ribose)-dependent recruitment of DNA repair enzymes.[3] Poly-ADP-ribosylation (PARylation) controls a wide variety of biological processes such as DNA damage response (DDR) and chromatin remodeling. PARP1 is the most abundant and active enzyme in the PARP family, and PARP-1 catalyzing DNA-dependent PARylation spearheaded the field of
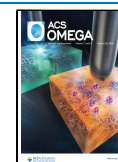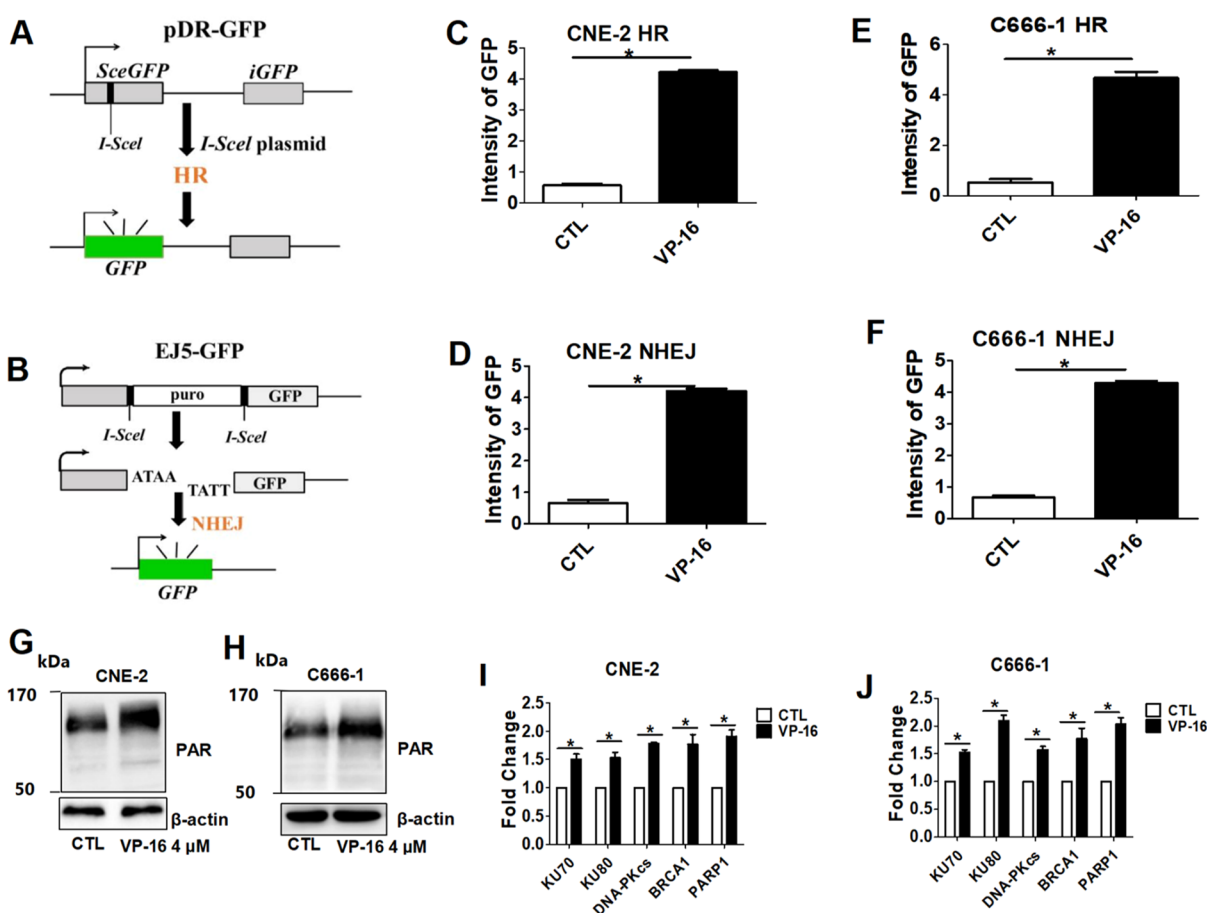
Figure 1. VP-16 induces DNA repair in NPC cells. (A) Diagram illustrating HR repair using DR-GFP transgenes. (B) Diagram illustrating NHEJ repair using EJ5-GFP transgenes derived from Wu, L. *Radiat Res.* **2013**, *179*(2), 160−170. https://doi.org/10.1667/RR3034.1. (C−F) Intensity of GFP in CNE-2 (C,D) and C666-1 (E,F) cells repaired by HR or NHEJ in response to I-SceI-generated DSBs, as determined using DR-GFP or EJ5-GFP reporter assays, respectively. Cells were treated with a vehicle or 4 μM VP-16 (10×). (G,H) Western blots showing PAR expression in CNE-2 and C666-1 cells. (I,J) Quantitative real-time polymerase chain reaction (qRT-PCR) detection of the expression of genes related to the HR and NHEJ pathways in CNE-2 (I) and C666-1 (J) cells. The data are presented as the mean ± SD of three independent experiments. *$P < 0.05$.

DDR.[11] The FDA has approved four PARP inhibitors. These inhibitors have transformed treatment for breast and ovarian cancers with BRCA mutations.[12] However, similar to other targeted therapies, resistance to PARPis has emerged in patients with advanced disease. A preclinical study has reported that a combination of high-dose PARPi and low-dose chemotherapy can inhibit the growth of tumor cells.[13] Ongoing clinical trials (e.g., NCT02049593; ClinicalTrials.gov) are evaluating the efficacy and tolerability of similar "high PARPi/low chemo" approaches. Moreover, PARP1 hyperactivation in DNA repair is crucial for resistance to genotoxic agents, which has been demonstrated in cell experiments, xenograft tumor models, and clinical studies.[14,15] In addition, PARP1 is overexpressed in NPC compared to normal nasopharyngeal cells.[3] Therefore, this study explored the possible use of the PARP1 inhibitor olaparib (Ola) as an NPC treatment.

A functional interaction between PARP and DNA-PK (DNA-PKcs) catalytic subunit has been reported.[16−18] DNA-PKcs, which is encoded by the PRKDC/XRCC7 gene, is a member of the phosphatidylinositol 3 (PI-3) kinase-like kinase (PIKK) family that plays a vital role in NHEJ.[19] DNA-PKcs expression correlates with a decreased therapeutic response to DNA-damaging agents in various cancers, indicating that DNA-PKcs-mediated DNA repair can promote cancer cell survival.[20,21] Moreover, DNA-PKcs levels are elevated in NPC and associated

with a shorter survival.[22] DNA-PKcs and PARP1 inhibitors are potential tools for anticancer therapeutic interventions.[18]

The DNA-PKcs and PARP1 activities are indispensable for the development of resistance to genotoxic agents; thus, we explored the regulatory interaction between these two DNA repair components in NPC. Ruscetti et al. showed that PARP is phosphorylated by purified DNA-PK, and the catalytic subunit of DNA-PK is ADP-ribosylated by PARP.[16] However, our work showed that DNA-PKcs and PARP1 undergo mutual regulation during etoposide-induced DNA repair in NPC.

By further exploring this mechanism, our work showed that a DNA-PKcs inhibitor combined with a PARP1 inhibitor results in robust synergy in NPC models both *in vivo* and *in vitro* by increasing DNA damage accumulation and reducing DNA repair efficacy, eventually inducing apoptosis.

■ RESULTS

VP-16 Activates DNA Repair in NPC Cells. VP-16 is a potent inducer of DSBs and promotes HR and NHEJ repair when used to treat cancers.[5,25] However, it is unknown whether VP-16 promotes DNA repair in NPC cells. Therefore, DR-GFP and EJ5-GFP reporter assays were used to measure DNA repair. The intensity of GFP increased dramatically, consistent with the fluorescence microscopy analysis shown in Figure S1, indicating that VP-16 promoted NHEJ and HR repair in both CNE-2 and
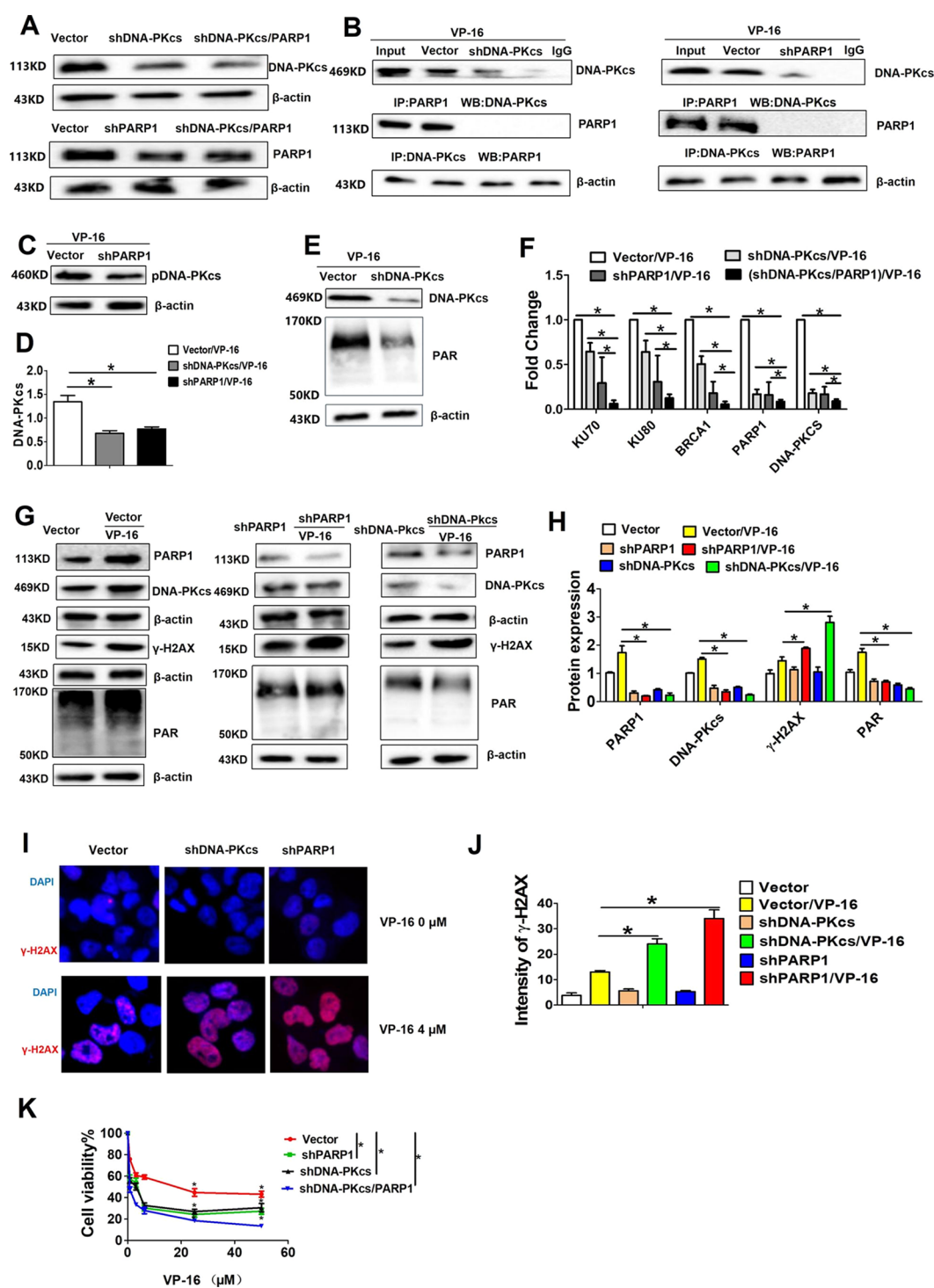
Figure 2. DNA-PKcs and PARP1 engage in a positive feedback to regulate DNA damage repair. (A) Efficiency of shRNAs was measured using western blotting. Cells were infected with Vector, PARP1 shRNA, and DNA-PKcs shRNA. shDNA-PKcs/PARP1 indicates that both DNA-PKcs and PARP1 were knocked down at the same time. (B) Coimmunoprecipitation was used to detect the interaction between DNA-PKcs and PARP1 in the cells after 4 h of 4 μM VP-16 treatment. (C) Phosphorylated DNA-PK at Ser2056 expression was detected by western blotting. (D) Content of DNA-PKcs after 4 h of 4 μM VP-16 treatment in PARP1-knockdown and DNA-PKcs-knockdown CNE-2 cells was examined using DNA-PKcs ELISAs. (E) Western blot showing PAR expression in cells expressing the control vector and shDNA-PKcs. (F) qRT-PCR detection of the expression of genes related to the BER, HR, and NHEJ pathways in DNA-PKcs-knockdown, PARP1-knockdown, and double-knockdown CNE-2 cells after 4 h of 4 μM VP-16 treatment. (G) Western blot validating PARP1, DNA-PKcs, PAR, and γ-H2AX expression in DNA-PKcs-knockdown and PARP1-knockdown CNE-2 cells treated as described in (F,G). (H) Statistical analysis of DNA-PKcs, PARP1, PAR, and γ-H2AX protein expressions in NPC cells. (I) γ-H2AX levels were determined using high-content imaging (20×). (J) Quantification of γ-H2AX levels in cells from three independent experiments. Cells were treated as described in (H). (K) shDNA-PKcs, shPARP1 and shPARP1/DNA-PKcs CNE-2 cells were treated with different concentrations of VP-16 (0−50 μM), and cell viability was evaluated using the MTT assay. The data are presented as the mean ± SD of three independent experiments. *$P <$ 0.05.
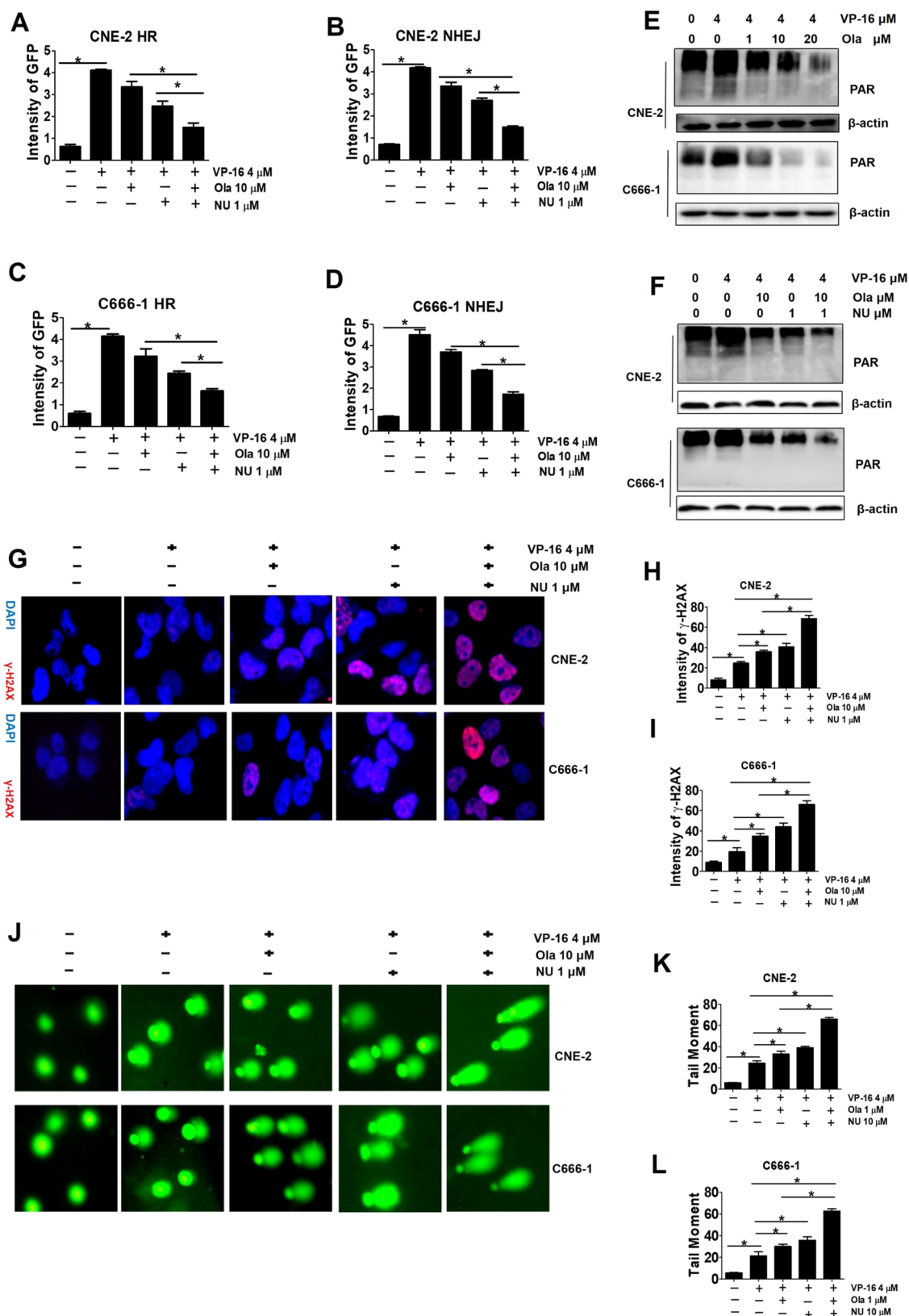
Figure 3. Cotreatment with Ola and NU increases DNA damage accumulation in NPC cells. (A−D) Percentage of GFP-positive cells repaired by the HR or NHEJ pathways. Cells were treated with vehicle, 4 μM VP-16, 10 μM Ola, or 1 μM NU alone or in combination. (E,F) PARylation in NPC cells expressing PAR, as detected using western blotting. (G−I) DNA damage (γ-H2AX) in CNE-2 cells after coadministration of Ola and NU, as determined using high-content imaging, 20×. (J−L) Neutral comet assays, 20×. *$P < 0.05$.

C666-1 NPC cells (Figure 1A−F). Moreover, PARylation was clearly induced by VP-16 in NPC cells (Figure 1G,H).

We evaluated the effects of the VP-16 treatment on the mRNA expression of KU70/80 (a DSB that serves to recruit
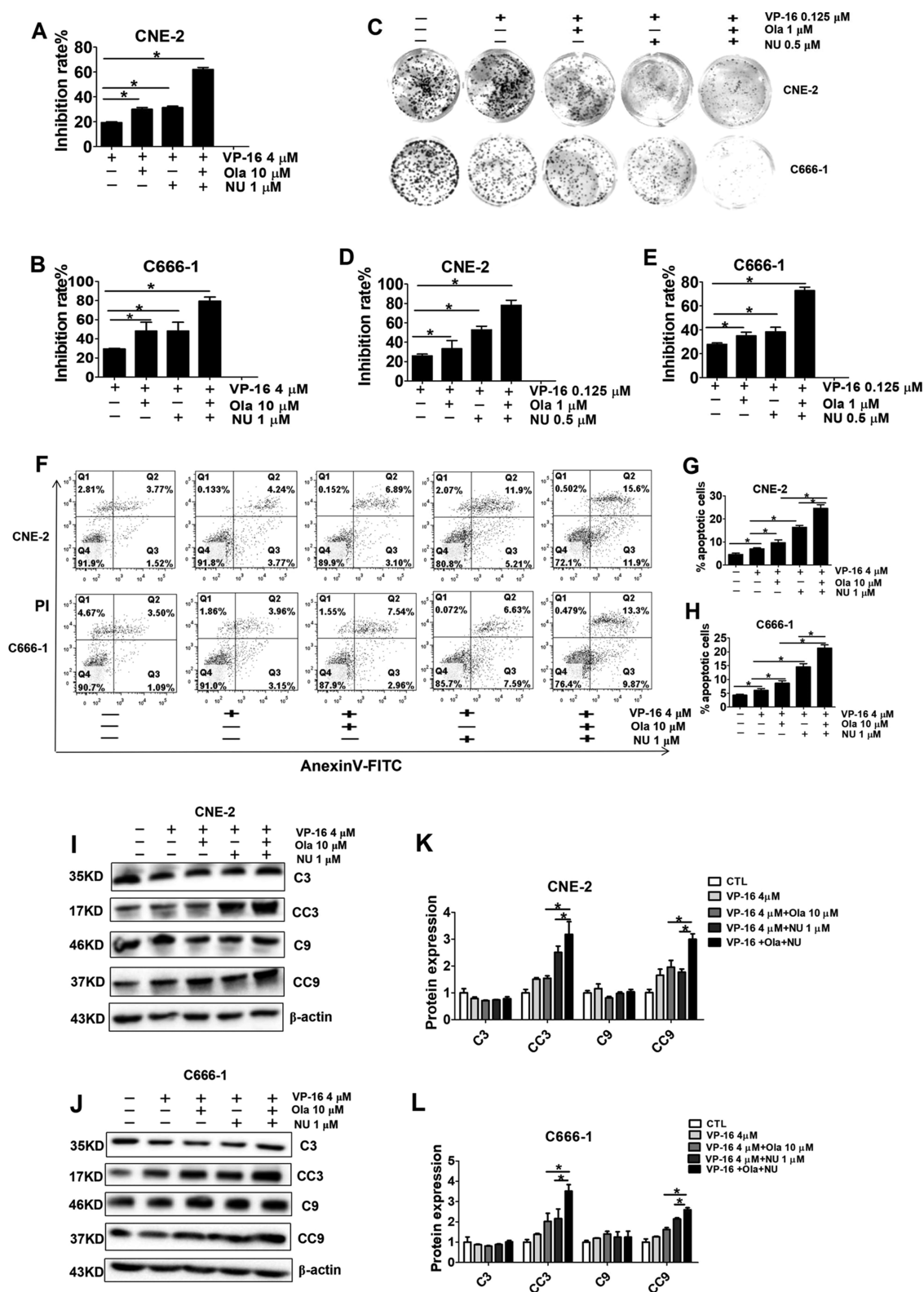
Figure 4. Dual inhibition of DNA-PKcs and PARP1 increases the efficacy of VP-16 in NPC cells. (A,B) CNE-2 and C666-1 cells were incubated with 4 μM VP-16, 10 μM Ola, and/or 1 μM NU for 72 h. Cell survival and proliferation were detected using MTT assays. The data are presented as the mean $\pm$ SE (n = 3) of the inhibition rate (%) relative to untreated control cells. (C,E) CNE-2 and C666-1 cells were incubated with 0.125 μM VP-16, 1 μM Ola, or 0.5 μM NU for 5 d, and the surviving fraction of control or treated cells was analyzed by performing clonogenic assays. The data are presented as the mean $\pm$ SE of three independent experiments. Representative images of the clonogenic assay are presented in (C). The percent inhibition is presented in bar graphs with error bars ($\pm$SE). (F) Flow cytometry images. (G,H) Quantitative analysis of the percentage of apoptotic cells after treatment with VP-16, Ola, and NU for 48 h. The percentage of total apoptotic cells is defined as the sum of the percentages of early and late apoptotic cells. (I,J) Western blot analysis of C3, CC3, C9, and CC9 levels in CNE-2 and C666-1 cells exposed to different concentrations of agents. (K,L) Statistical analysis of C3, CC3, C9, and CC9 levels in NPC cells.

other NHEJ proteins in order to strengthen the joining of DNA ends),[26] BRCA1 (BRCA1 is essential for the repair DSB and stalled replication forks via HR pathway),[13] DNA-PKcs and PARP1, which are major factors involved in NHEJ, HR, and BER, to elucidate the mechanisms underlying the VP-16-mediated activation of DNA repair pathways. As shown in Figure 1I,J, VP-16 increased the mRNA expression of all these factors, indicating that VP-16 activated multiple DNA repair pathways in NPC cells. These changes may account for NPC cell resistance to VP-16.

DNA-PKcs and PARP1 Undergo Mutual Interactions to Regulate VP-16-Induced DNA Damage Repair. Both DNA-PKcs and PARP1 activities are indispensable for the development of resistance to genotoxic agents;[3,18] thus, we explored the regulatory interaction between these two DNA repair components. Then, we constructed DNA-PKcs-knockdown and PARP1-knockdown CNE-2 cells by transfecting a lentiviral shRNA (Figure 2A) to gain additional insights into the mechanisms by which DNA-PKcs and PARP1 regulate VP-16-induced DNA repair in NPC cells. The target sequences of the lentiviruses are listed in Table S2. We knocked down PARP1 and/or DNA-PKcs in CNE-2 cells treated with 4 μM VP-16 to investigate the interaction between these two enzymes by performing immunoprecipitation. IgG and input were employed as negative and positive controls, respectively. Through immunoprecipitation experiments, we observed a direct association between DNA-PKcs and PARP1 (Figure 2B). Then, we knocked down PARP1 in CNE-2 cells and assessed the effects on DNA-PKcs activities after DNA damage to determine whether PARP1 can play a vital role in DNA-PKcs activation upon DNA damage in NPC cells (Figure 2C). The level of DNA-PK phosphorylated at Ser2056 (a marker of DNA-PK activation) was significantly reduced.[27,28] Thus, PARP1 knockdown could reduce DNA-PKcs activities during DNA repair (Figure 2C). We also found that the DNA-PKcs expression was inhibited in PARP1-knockdown CNE-2 cells treated with 4 μM VP-16 for 4 h by the enzyme-linked immunoassay (ELISA) (Figure 2D).

Next, we detected the level of PARylation in cells with DNA-PKcs knockdown after DNA damage, and the level was obviously reduced (Figure 2E). Although some reports have documented PARP1-mediated PARylation of DNA-PKcs,[16] our results showed the opposite effect, that is, DNA-PKcs regulated PARP1 activity in the DDR.

In addition, we detected the mRNA and protein expression of DNA-PKcs and genes related to DNA repair pathways (BER, NHEJ, and HR) using qRT-PCR and western blotting, respectively, in PARP1-knockdown CNE-2 cells to obtain additional insights into the mechanism by which PARP1 regulates DNA-PKcs (Figure 2F–H). The results showed significantly decreased DNA-PKcs mRNA and protein levels in PARP1-knockdown CNE-2 cells. Conversely, because DNA-PKcs is a transcription factor, we sought to explore the exact role of DNA-PKcs in modulating PARP1 transcription. As a result, the expression levels of the related genes KU70, KU80, PARP1, and BRCA1 were also lower when DNA-PKcs was down-regulated in CNE-2 cells treated with VP-16 for 4 h (Figure 2F–H). Therefore, DNA-PKcs and PARP1 interfere with each other, indicating that these two proteins engage in a positive feedback mechanism of DNA repair in NPC cells.

We knocked down DNA-PKcs and PARP1 separately in CNE-2 cells and then treated the cells with VP-16 to assess the individual roles of DNA-PKcs and PARP1 in DNA damage

accumulation in NPC cells. γ-H2AX was used as an indicator of DNA DSBs.[29] The western blot results (Figure 2G,H) showed a considerable increase in the γ-H2AX expression in CNE-2 cells after treatment with VP-16 for 4 h. However, cells with PARP1 or DNA-PKcs knockdown exhibited higher γ-H2AX levels, consistent with the fluorescence microscopy analysis shown in Figure 2I,J. Next, a concurrent knockdown of PARP1 and DNA-PKcs rendered cells more sensitive to VP-16 than the knockdown of either gene alone (Figure 2K). Based on these results, the simultaneous targeting of this positive feedback mechanism through simultaneous DNA-PKcs and PARP1 inhibition results in a more pronounced therapeutic effect than the inhibition of a single target.

Ola and NU Synergistically Inhibit VP-16-Induced DNA Repair. NU and Ola, which are the small-molecule inhibitors of DNA-PKcs and PARP1/2, respectively,[30,31] were used to validate the mechanism underlying the positive interaction between PARP1 and DNA-PKcs, and the possibility of clinical translation. We found that 4 μM VP-16 promoted DNA repair (Figure 1). Unexpectedly, Ola treatment only slightly decreased HR and NHEJ, whereas 1 μM NU treatment significantly reduced HR and NHEJ (Figure 3A–D). We also evaluated the PAR expression in NPC cells exposed to VP-16 and various concentrations of Ola (0–20 μM). PARylation was induced by VP-16 in NPC cells but was inhibited by both Ola and NU (Figure 3E,F). The quantification of PAR is shown in Figure S3.

The combination of Ola and VP-16 was unable to effectively inhibit DNA repair in NPC cells. However, cotreatment with (10 μM) Ola and (1 μM) NU significantly disrupted HR and NHEJ and inhibited the PARylation induced by VP-16.

Ola increases the accumulation of DNA damage in NPC cells, consistent with previous reports.[32,33] NU promotes the accumulation of DNA damage by blocking DNA repair. Thus, we monitored the clearance of γ-H2AX in NPC cells and found that coadministration of Ola and NU remarkably induced the accumulation of VP-16-induced DNA damage in NPC cells (Figure 3G–I). These findings are consistent with the comet assay results (Figure 3J–L). Collectively, our study indicates that pharmacological inhibition of DNA-PKcs and PARP1 can jointly block DNA repair.

Cotreatment with Ola and NU Significantly Inhibits NPC Cell Proliferation and Promotes VP-16-Induced Apoptosis. Because the inhibition of PARP1 or DNA-PKcs increased DNA damage, MTT assays were performed to measure changes in CNE-2 and C666-1 cell proliferation after treatment with different concentrations of VP-16, Ola, and NU and to determine whether the combination of Ola and NU sensitizes NPCs to VP-16. Cotreatment with Ola and NU dramatically potentiated the effect of VP-16 on NPC cell growth inhibition (Figure 4A,B). The cytotoxicity of VP-16, Ola, NU, VP + Ola, and VP + NU toward NPC cells is shown in Figure S2. Next, we validated these observations using colony-formation assays. Ola combined with NU markedly increased the inhibitory effect of VP-16 on colony formation, whereas VP-16 alone only exerted slight effects on both cell lines after 5 d of exposure. These results indicated the synergistic effects of concurrent Ola and NU treatment on NPC cell proliferation (Figure 4C–E).

Annexin V-FITC/PI staining and western blot analysis were conducted to ascertain whether the increased response to VP-16 observed *in vitro* was associated with apoptosis. Annexin V-FITC/PI staining showed that both Ola and NU alone increased
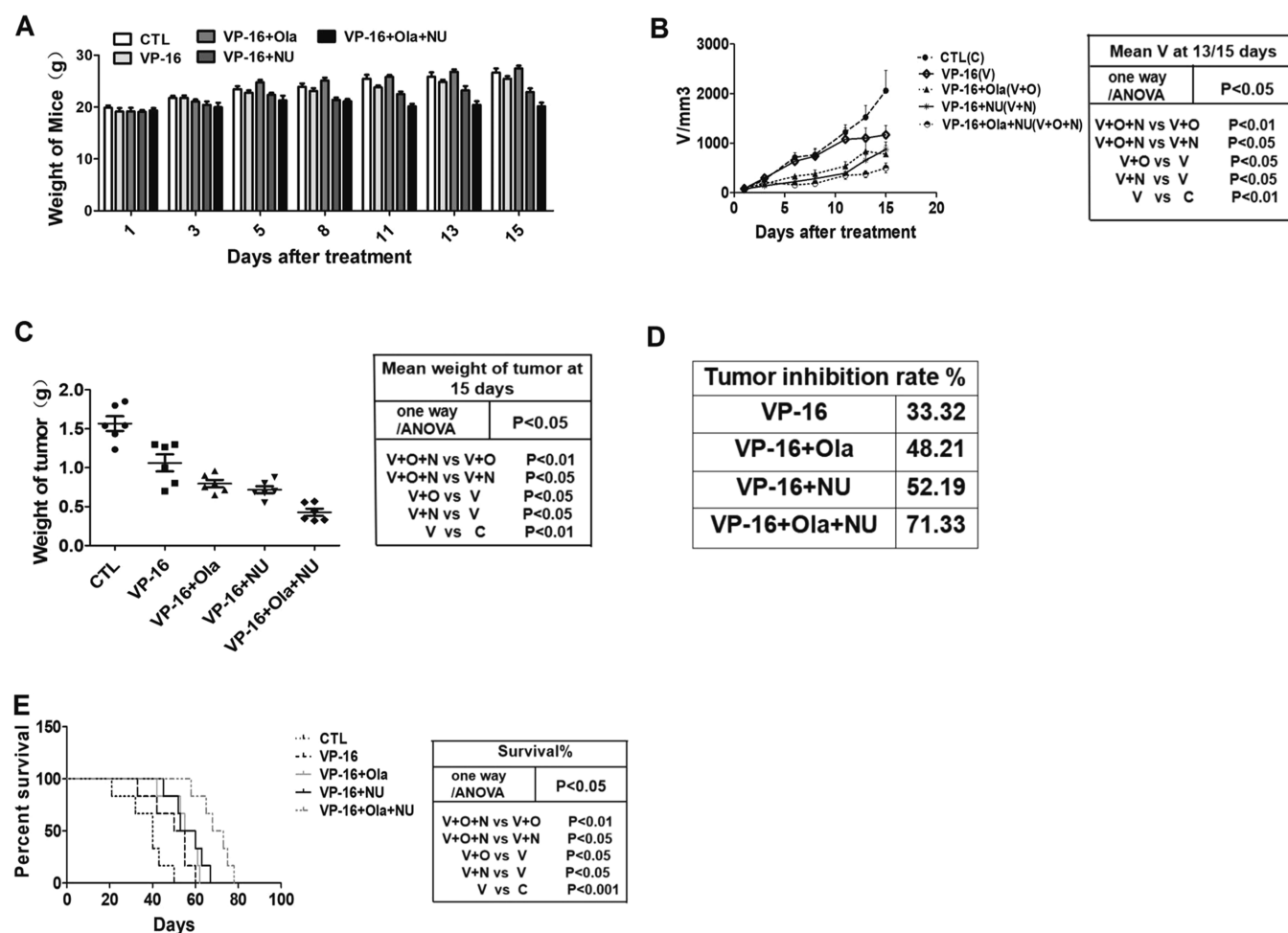
Figure 5. Ola plus NU enhances the antitumor effects of VP-16 on a CNE-2 xenograft model in mice. A mouse xenograft model was established with CNE-2 cells. The mice were treated with 10 mg/kg VP-16 (injected i.p., $n = 6$), 10 mg/kg VP-16 plus 50 mg/kg Ola (injected i.p., $n = 6$), 10 mg/kg VP-16 plus NU (injected i.p., $n = 6$), 10 mg/kg VP-16 plus 50 mg/kg Ola, and 10 mg/kg NU (injected i.p., $n = 6$), or CTL (injected i.p., $n = 6$) daily for 15 d. (A) Relative body weights of recipient mice in each group during treatment for 15 d. (B) Tumor volume in each mouse was measured three times a week during treatment for 15 d. (C) Tumor weight was measured in mice with CNE-2 xenografts, and the statistical significance of differences among the four groups was analyzed using one-way ANOVA and the Tukey−Kramer method. (D) Tumor inhibition rate (%) in different drug treatment groups. (E) Kaplan−Meier survival analysis of each group of mice. Survival times: CTL (40 d), VP-16 (50 d), VP-16 + Ola (53 d), VP-16 + NU (58 d), and VP-16 + Ola + NU (62 d).

VP-16-induced apoptosis, whereas the combined treatment further elevated the apoptotic rate at 48 h after DSB induction (Figure 4F−H). Furthermore, the western blotting results were consistent with the results from this experiment, as indicated by the increased CC3 and CC9 levels (Figure 4I−L).

Dual Inhibition of DNA-PKcs and PARP1 Potentiates the Antitumor Effect of VP-16 in Mouse Xenograft Models. Based on the *in vitro* observation, we further investigated whether the dual inhibition of DNA-PKcs and PARP1 can improve the anticancer efficacy of VP-16 *in vivo*. We established a mouse xenograft model using CNE-2 cells. Xenograft tumor growth was slightly inhibited in the VP-16 treatment group compared to the control group, and only a slight change in the response to VP-16 (10 mg/kg, i.p., $n = 6$) was observed upon the addition of Ola (50 mg/kg, i.p., $n = 6$) or NU (10 mg/kg, i.p., $n = 6$). In the group treated with VP-16, Ola, and NU (i.p., $n = 6$), the antitumor effect was significantly increased (Figure 5). After treatment for 15 d, no obvious difference in body weight was noted (Figure 5A). Tumor volume was measured three times a week during treatment. CNE-2 xenograft tumor could grow rapidly in the untreated

group. VP-16 treatment alone and in combination with either Ola or NU slightly reduced tumor growth. On the contrary, the combination of VP-16, Ola, and NU markedly reduced tumor volume and weight (Figure 5B,C). The tumor inhibition rate was consistent with the results described above (Figure 5D). The survival time analysis showed that VP-16 alone exerted a slight effect on median survival (50 vs 43 d), whereas combination treatment with Ola (53 vs 50 d) or NU (58 vs 50 d) increased the efficacy of VP-16 somewhat. Furthermore, the simultaneous administration of all three drugs showed a significant survival benefit compared to the administration of two-drug combinations (62 vs 58/53 d; Figure 5E).

■ DISCUSSION

Here, we provide evidence of a mutual interaction between DNA-PKcs and PARP1 in the presence of a DNA-damaging agent. Moreover, to identify the mechanism underlying the regulation of these two enzymes, NPC cells were transfected with shRNA control (vector), DNA-PKcs-RNAi (shDNA-PKcs), or PARP1-RNAi (shPARP1) to knockdown DNA-PKcs and/or PARP1. Ariumi et al. clarified that DNA-PK could

suppress PARP activity, possibly through direct binding and/or sequestration of DNA ends.[17] However, DNA-PKcs knockdown or inhibition reduced PARylation in DNA-damaged NPC cells in our study, perhaps at least in part due to the modulation of PARP1 gene transcription. Conversely, PARP1 knockdown reduced DNA-PKcs activity and expression, as evidenced by decreased levels of the DNA-PKcs mRNA and the DNA-PKcs protein phosphorylated at Ser2056 (Figure 2). Based on these results, DNA-PKcs and PARP1 engage in a positive feedback mechanism during DNA repair. This new interaction complements the DNA damage and repair mechanisms involving DNA-PKcs and PARP1 after exposure to a DNA-damaging agent. These findings, which we validated in NPC cell lines, could translate into improved NPC treatment strategies.

Much effort has been devoted to solving problems relating to tumor recurrence and drug resistance. Alterations in DNA repair have been observed in drug-resistant tumor cells.[7,34] BER, through PARP1 activity, is responsible for the repair of DNA single-strand breaks (SSBs). The suppression of PARP1 activity markedly delays SSB repair, which leads to the formation of DSBs upon collision with an ongoing replication fork. These DSBs are mainly and efficiently repaired by HR and NHEJ.[7,33] An understanding of the activities of various DNA repair pathways in each tumor and the association of DNA repair functions with drug responses is crucial to patient selection for treatment with agents targeting DNA repair.[3,30] In the present study, the HR and NHEJ repair pathways and PARylation were induced by VP-16 (Figure 1). Therefore, blocking only one of these pathways may not be sufficient to prevent VP-16 resistance. However, an elucidation of multiple DNA repair pathways and mechanisms can provide an effective strategy for sensitizing cancer cells to drug treatment. The mechanisms of intracellular repair are relatively complex, and the disruption of one repair pathway can induce the compensatory activation of other repair pathways, which in turns lead to an incomplete DNA repair inhibition. Similar to other targeted therapies, the majority of with advanced cancer develop acquired resistance to PARPis.[35] Several PARPis resistance mechanisms have been determined via *in vitro* experiments, including the inactivation of DNA repair proteins.[35] Several studies have also indicated that dysfunctional NHEJ is crucial for forming genomic instability in PARPi-treated cells,[11] and DNA-PKcs inhibition can lead to HR functional recovery and PARPi resistance *in vitro*.[12]

In our study, we used Ola (a specific inhibitor of PARP1/2) and NU (a specific inhibitor of DNA-PKcs)[30,31] to verify the mechanisms of the positive feedback between DNA-PKcs and PARP1, and their potentials for clinical translation. Therefore, only the simultaneous inhibition of multiple pathways will obtain superior therapeutic effects. Ola in combination with VP-16 inhibited BER-mediated DNA repair by suppressing PARylation in our study. Nonetheless, the HR and NHEJ repair efficacy was only slightly decreased when PARP activity was inhibited by Ola (Figure 3). Notably, HR and NHEJ were significantly blocked by the combination of Ola and NU. This phenomenon may be due to the significant interaction, crosstalk, and overlap among DNA repair pathways in response to various types of DNA damage.[36] The interplay between DNA-PK and PARP1 appears quite complex. Several studies have demonstrated an interaction between the two enzymes;[37–40] while other studies imply the distinct roles of these proteins in regulating a NHEJ DNA repair pathway.[41,42] Laura, et al. reported that DNA-PK and PARP1 lack additivity in the cellular response to clinically relevant radiation doses by assessing DNA

DSB repair.[43] Recently, AZD7648 was identified as a DNA-PK inhibitor that promotes the activities of radiotherapy, chemotherapy, and olaparib to achieve better responses to current therapies.[44] The study by Zeng et al. also revealed that the combination of PARP and DNA-PK inhibitors with IR suppresses the growth of HPV-negative head and neck cancer squamous carcinoma *in vitro* and *in vivo*.[45] The combined inhibition of PARP and DNA-PK without IR is currently being evaluated in a clinical trial (NCT03907969). According to Han et al., the synergistic inhibition of PARylation and DNA-PK activity promotes cell death.[27] In the present study, a positive feedback regulation of PARP1 and DNA-PKcs altered the sensitivity of NPC cells to VP-16, and the efficacy of PARP1 and DNA-PKcs inhibitor therapies was modulated by these relationships among DNA repair pathways during VP-16-induced DNA repair. Therefore, cotreatment with Ola and NU simultaneously inhibits HR and NHEJ.

Finally, the simultaneous administration of these three drugs inhibited NHEJ, HR, and PARylation (Figure 3A−F), increased DNA damage accumulation (Figure 3G−L), decreased DNA repair, and induced apoptosis. All of these changes subsequently resulted in reduced NPC cell proliferation (Figure 4), increased survival, and delayed disease progression in a NPC xenograft tumor model (Figure 5).

CONCLUSIONS

In summary, elucidating the molecular mechanisms of cancer resistance to VP-16 is of great importance because the effectiveness of VP-16 therapy is limited by its high dose and subsequent adverse events in patients with recurrent disease.[46] This study provides consistent evidence that DNA repair contributes to VP-16 resistance. The findings inspired us to use DNA-PKcs and PARP1 inhibitors to potentiate the effect of VP-16. Moreover, we found that NPC cells exhibit different responses to Ola and NU when administered alone or in combination. Combined treatment with PARP1 and DNA-PKcs inhibitors significantly inhibited cell growth by blocking multiple DNA repair pathways. The combination of PARP1 and DNA-PKcs inhibitors leads to cell apoptosis, thereby promoting the cytotoxic effect of VP-16. This combination may help to reduce the doses of both compounds and therefore diminish the side effects associated with these agents. Our investigation provides new insights into combination drug therapies for NPC. Finally, this concept may broaden the application of Ola in cancer treatment.

MATERIALS AND METHODS

Reagents. Ola and VP-16 were purchased from Shanghai Biobond and Qilu Pharmaceuticals (Shanghai, China), respectively. NU7441 (NU) was supplied by Selleck (TX, USA). Ola and NU were dissolved in dimethyl sulfoxide (DMSO) to prepare stock solutions (10 mmol/L).

Transfection. shRNAs were constructed by GenePharma (Shanghai, China). CNE-2 cells were transfected with the shRNA control (Vector), DNA-PKcs-RNAi (shDNA-PKcs), or PARP1-RNAi (shPARP1) using LipoFiter3 (Hanbio #HB-LF3-1000) as per the manufacturer's instructions. After transfection for 48 h, the cells were harvested for subsequent experiments.

Cell Lines and Culture. Human NPC cells (C666-1 and CNE-2) authenticated by short tandem repeat analysis were provided by Fujian Provincial Cancer Hospital. All cells were stored and passaged for <2 months prior to the experiments and

maintained in RPMI 1640 (Thermo Fisher Scientific Inc., MA, USA) containing 10 μg/mL gentamicin (Cellgro, VA, USA) and 10% FBS (Welgene Inc., Daegue, South Korea) at 37 °C and 5% CO_2.

MTT Assay. CNE-2 and C666-1 NPC cells (3000 cells/well) were grown in 96-well plates. The cytotoxicity of the test compounds was assessed by the MTT assay. After treatment for 72 h, the MTT solution was added and incubated at 37 °C for 4 h. The resulting formazan crystals were dissolved in DMSO, and the absorbance was measured using a multifunctional microplate reader at 570 nm.

Colony-Formation Assay. The effect of NU on CNE-2 and C666-1 cell viability in the presence of VP-16 and Ola was measured using a colony-formation assay. CNE-2 and C666-1 cells (500 cells/well) were inoculated into 12-well plates. After overnight incubation, the control and experimental groups (0.125 μM VP-16, 0.125 μM VP-16 plus 1 μM Ola, and 0.125 μM VP-16 plus 0.5 μM NU with or without Ola) were further incubated for 5 d, followed by crystal violet (0.1%) staining. Colonies with more than 50 cells were counted. The survival rate was determined relative to the number of colonies in the control group.

Western Blot Analysis. The levels of PAR, PARP1, DNA-PKcs, Caspase 3 (C3), Caspase 9 (C9), Cleaved C3 (CC3), Cleaved C9 (CC9), γ-H2AX, and β-actin in NPC cells were examined using western blotting. The following primary antibodies were used as follows: anti-PAR (Calbiochem #AM80, 100 μL); anti-PARP1 (Abcam #ab194586, 100 μL); anti-DNA-PKcs (Abcam #ab1832, 100 μg); anti-pSer2056 DNA-PKcs (Abcam #ab18192, 100 μg); anti-C3 (CST #9662, 100 μL); anti-C9 (CST #9508, 100 μL); anti-CC3 (CST #9661, 100 μL); anti-CC9 (CST #7237, 20 μL); antiγ-H2AX (CST #9718, 100 μL); and anti-β-actin (Abcam #ab227387, 100 μL). Goat anti-mouse (Proteintech #SA00001-1, 100 μL) or anti-rabbit (Proteintech #SA100001-2, 100 μL) secondary antibodies were used. The cells were lysed on ice for 20 min in NP-40 lysis buffer containing 1× PMSF, phosphatase inhibitors, and protease inhibitors. Protein lysates were separated on Bis—Tris gels and then transferred onto PVDF membranes (Millipore, USA). After blocking with 5% milk for 1 h, the membranes were incubated with diluted antibodies overnight at 4 °C, and then with secondary antibodies (Abcam, Cambridge, UK) at room temperature before the protein bands were visualized with enhanced chemiluminescence (Beyotime Biotechnology, MA, USA). Data analysis was conducted using ImageJ software.

Annexin V-FITC/PI Double Staining. The cells (1×10^6 cells/mL) were grown in 6-well plates and treated with 4 μM VP-16, 1 μM NU, and/or 10 μM Ola for 48 h. After staining with an annexin V-FITC/PI dual fluorescence apoptosis detection kit (BioUniquer Technology), the samples were detected using a FACSCalibur flow cytometer (FACSAria II, Becton Dickinson) within 1 h of staining.

Comet Assay. A total of 2.5×10^5 NPC CNE-2 and C666-1 cells were exposed to 4 μM VP-16, 1 μM NU, and/or 10 μM Ola for 12 h. Subsequently, the cells were collected and analyzed with a CometAssay kit from #ADI-900-166, Trevigen Gaithersburg, MD, USA. Approximately 100 images of nuclei from cells on each slide were captured, and the tail moments and relative % DNA in the comet tail were measured with CASP software.

γ-H2AX Foci Assay. NPC cells were grown and treated with drugs (4 μM VP-16, 1 μM NU and/or 10 μM Ola) for 12 h. After fixing, rupturing, and blocking sequentially, the cells were

incubated with primary and secondary antibodies. To identify γ-H2AX foci, the anti-H2AX mouse monoclonal antibody (1:1000, Abcam) were detected using a high content imaging system (Thermo Fisher, USA). Hoechst 33342 (#BB-4135-1, BestBio, Shanghai, China) was used to counterstain the nuclei. Quantification was performed with quantitative software for an inverted fluorescence microscope.

HR/NHEJ Assay. The NHEJ and HR assays were carried out as described in a previous publication with some modifications.[23] The pDR-GFP, EJ5-GFP, and pCBASceI plasmids were obtained from Addgene (Seoul, South Korea). Transient expression of the rare homing restriction enzyme I-SceI in NPC cells that carry the pDR-GFP plasmid produced a DSB in one of two mutant GFP genes (SceGFP and iGFP) (Figure 1A). DSBs can be repaired by HR between the two mutant GFP genes, thus leading to the recovery of the GFP gene and expression of the GFP protein. As shown in Figure 1B, EJ5-GFP consists of a promoter separated from the GFP coding sequences by the puromycin (puro) gene. The promoter can be linked to the remaining part of the cassette to restore GFP gene when the puro gene is removed by NHEJ-mediated repair of the two I-SceI-induced DSBs. Thus, the quantification of the percentage of GFP-positive cells can determine the efficiency of HR- and NHEJ-mediated DSB repair. The pDR-GFP and EJ5-GFP plasmids were transfected into CNE-2 and C666-1 cells, which were infected with the pCBASceI plasmid 2 d later. After transfection for 6 h, the cells were exposed to 4 μM VP-16, 10 μM Ola, or 1 μM NU. If the cells were able to activate the HR/NHEJ pathways, GFP was expressed, and the rate of GFP positivity was detected with ImageJ software (NIH, Bethesda, MD, USA).

qRT-PCR. Total RNA was extracted from cultured cells using a BIOzol reagent (#BSC52M1, BioFlux). Reverse transcription was performed with an Advantage RT-for-PCR Kit (Takara, Dalian, China). A two-step PCR system (Applied Biosystems, NY, USA) was used for qRT-PCR (SYBR Green was supplied by Sigma-Aldrich, MO, USA), and a quantitative comparative analysis of the threshold cycle (Ct) was performed.[24] The following thermal cycling conditions were used: 30 s at 95°, followed by 35 cycles of 10 s at 95 °C, 32 s at 60 °C, 15 s at 95 °C, 60 s at 60 °C, and 15 s at 95 °C. All primer sequences used for qRT-PCR are presented in Table S1.

DNA-PKcs ELISA. A DNA-PKcs Cell-Based ELISA Kit (#LS-F1945, LSBio) was employed by following the manufacturer's protocol. The protein content of DNA-PKcs was assessed by measuring the absorbance values at 570 nm using the multifunctional microplate reader.

Immunoprecipitation. First, 10—30 μL of a 50% protein A agarose bead suspension was added to 200 μL of the cell lysate (1 mg/mL), and this mixture was incubated at 4 °C for 0.5—1.0 h. Then, 5 μg of DNA-PKcs antibody, PARP1 antibody, or normal rabbit IgG was added to the cell lysate mixture and incubated overnight at 4 °C. After washing four times with 500 μL of cell lysis buffer, the pellets were resuspended in 20 μL of the 3× SDS sample buffer, vortexed, centrifuged, and denatured. Finally, the samples were analyzed using western blotting according to the detailed procedure described above.

***In Vivo* Study.** All animal experiments complied with the Animal Research: Reporting *In Vivo* Experiments Guidelines and were conducted at the Experimental Animal Center of Fujian Medical University (Fuzhou, China) in compliance with the guidelines after obtaining approval from the Institutional Animal Care and Use Committee (no. 2017-046).

Thirty BALB/c athymic nude mice (female, 5 weeks old) were supplied by the Experimental Animal Center of Shanghai Shrike. NPC cells (1×10^6) were injected subcutaneously into the right flanks of the mice. After the transplanted tumors grew to at least 100 mm^3, the animals were randomly assigned to five different groups for drug administration ($n = 6$ per group): the CTL group (PBS); the VP-16-only group (10 mg/kg in PBS, i.p.); the VP-16 plus Ola group (Ola, 50 mg/kg in PBS, i.p.); the VP-16 plus NU group (NU, 10 mg/kg in PBS); and a three-drug combination group (10 mg/kg VP-16, 50 mg/kg Ola, and 10 mg/kg NU). When the tumors of the mice in the control group reached 2000 mm^3, the experiment was terminated. The mice were treated daily for 15 d. The tumor volume was measured using the equation $[(\text{width}) 2 \times (\text{height})]/2$. Tumor size and mouse body weight were measured three times weekly. The survival time was recorded and analyzed using the Kaplan−Meier approach and log-rank test (GraphPad Prism software).

Statistical Analysis. All values are shown as mean ± standard error (SD). Significant differences were determined by Student's *t*-test (parametric) for *in vitro* studies to compare two groups of independent samples. ANOVA for *in vivo* studies was employed to assess the statistical significance among multiple groups. Level of statistical significance was set at $P < 0.05$, indicated by *. All statistical tests were conducted with GraphPad Prism software (GraphPad, CA, USA).

■ ASSOCIATED CONTENT

Ⓢ Supporting Information

The Supporting Information is available free of charge at https://pubs.acs.org/doi/10.1021/acsomega.1c04379.

Fluorescence microscopy analysis of HR and NHEJ repair after treatment with VP-16 in Figure 1, effects of Ola and NU on NPC cells cultured in the presence or absence of VP-16, quantification of PAR with CNE-2 and C666-1 cells in Figure 3E,F, primer sequences for qRT-PCR, and target sequences of lentivirus (PDF)

■ AUTHOR INFORMATION

Corresponding Authors

Lixian Wu − *Department of Pharmacology, School of Pharmacy, Fujian Medical University (FMU), Fuzhou 350005, P. R. China; Fujian Key Laboratory of Natural Medicine Pharmacology and Institute of Materia Medical, Fujian Medical University (FMU), Fuzhou 350005, P. R. China;* ⓞ orcid.org/0000-0001-6505-0648; Phone: 86-591-22862016; Email: wlx-lisa@fjmu.edu.cn

Ying Wu − *Key Laboratory of Natural Drug Pharmacology in Fujian Province, School of Pharmacy, Fujian Medical University, Fuzhou 350122, P. R. China;* Phone: 86-591-22862016; Email: wy@fjmu.edu.cn

Authors

Lingyu Zhang − *Fujian Medical University Cancer Hospital, Fujian Cancer Hospital, Fuzhou 350001, China; Fujian Key Laboratory of Translational Cancer Medicine, Fuzhou 350001, China; Department of Pharmacology, School of Pharmacy, Fujian Medical University (FMU), Fuzhou 350005, P. R. China; Fujian Key Laboratory of Natural Medicine Pharmacology, Fujian Medical University (FMU), Fuzhou 350005, P. R. China*

Yingting Zhuang − *Department of Pharmacology, School of Pharmacy, Fujian Medical University (FMU), Fuzhou 350005, P. R. China*

Guihui Tu − *Department of Pharmacology, School of Pharmacy, Fujian Medical University (FMU), Fuzhou 350005, P. R. China*

Ding Li − *Department of Pharmacy, Affiliated Cancer Hospital of Zhengzhou University, Henan Cancer Hospital, Zhengzhou 450008, P. R. China*

Yingjuan Fan − *Department of Pharmacology, School of Pharmacy, Fujian Medical University (FMU), Fuzhou 350005, P. R. China*

Shengnan Ye − *The First Affiliated Hospital of Fujian Medical University, Fuzhou 350004, China*

Jianhua Xu − *Department of Pharmacology, School of Pharmacy, Fujian Medical University (FMU), Fuzhou 350005, P. R. China; Fujian Key Laboratory of Natural Medicine Pharmacology and Institute of Materia Medical, Fujian Medical University (FMU), Fuzhou 350005, P. R. China*

Ming Zheng − *Fujian Key Laboratory of Natural Medicine Pharmacology, Fujian Medical University (FMU), Fuzhou 350005, P. R. China*

Complete contact information is available at:
https://pubs.acs.org/10.1021/acsomega.1c04379

Author Contributions

Conception and design: L.Z., Y.W., L.W., and Y.Z. Development of methodology: L.Z., Y.Z., G.T., and D.L. Acquisition of data (provided animals, acquired and managed patients, provided facilities, etc.): L.Z., G.T., and D.L. Analysis and interpretation of data (e.g., statistical analysis, biostatistics, and computational analysis): L.Z. and Y.F. Writing, review, and/or revision of the manuscript: L.Z. and L.W. Administrative, technical, or material support (i.e., reporting or organizing data and constructing databases): L.W., J.X., M.Z., and S.Y. Study supervision: Y.W. and L.W.

Notes

The authors declare no competing financial interest.

■ ACKNOWLEDGMENTS

■ REFERENCES

(1) Li, Y.; Yang, X.; Du, X.; Lei, Y.; He, Q.; Hong, X.; Tang, X.; Wen, X.; Zhang, P.; SUN, Y.; Zhang, J.; Wang, Y.; Ma, J.; Liu, N. RAB37 Hypermethylation Regulates Metastasis and Resistance Docetaxel-Based Induction Chemotherapy in Nasopharyngeal Carcinoma. *Clin. Cancer Res.* **2018**, *24*, 6495−6508.

(2) Mao, Y.-P.; Xie, F.-Y.; Liu, L.-Z.; Sun, Y.; Li, L.; Tang, L.-L.; Liao, X.-B.; Xu, H.-Y.; Chen, L.; Lai, S.-Z.; Lin, A.-H.; Liu, M.-Z.; Ma, J. Re-

evaluation of 6th edition of AJCC staging system for nasopharyngeal carcinoma and proposed improvement based on magnetic resonance imaging. *Int. J. Radiat. Oncol., Biol., Phys.* **2009**, *73*, 1326−1334.

(3) Chow, J. P. H.; Man, W. Y.; Mao, M.; Chen, H.; Cheung, F.; Nicholls, J.; Tsao, S. W.; Li Lung, M.; Poon, R. Y. C. PARP1 is overexpressed in nasopharyngeal carcinoma and its inhibition enhances radiotherapy. *Mol. Cancer Ther.* **2013**, *12*, 2517−2528.

(4) Xiang, Y.-Q.; Min, H. Q.; Hong, M. H.; Cao, S. M.; He, J. H.; Hou, J. H. Expression of Topoisomerase IIα in Nasopharyngeal Carcinoma and its Clinical Significance. *Chin. J. Cancer* **2004**, *23*, 322−325.

(5) Wijdeven, R. H.; Pang, B.; van der Zanden, S. Y.; Qiao, X.; Blomen, V.; Hoogstraat, M.; Lips, E. H.; Janssen, L.; Wessels, L.; Brummelkamp, T. R.; Neefjes, J. Genome-Wide Identification and Characterization of Novel Factors conferring resistance to Topoisomerase II Poisons in Cancer. *Cancer Res.* **2015**, *75*, 4176−4187.

(6) Biasoli, D.; Kahn, S. A.; Cornélio, T. A.; Furtado, M.; Campanati, L.; Chneiweiss, H.; Moura-Neto, V.; Borges, H. L. Retinoblastoma protein regulates the crosstalk between autophagy and apoptosis, and favors glioblastoma resistance to etoposide. *Cell Death Discovery* **2013**, *4*, No. e767.

(7) Rodrigues, A. S.; Bruno, C. G.; Marta, G.; Oliverira, N. G.; Guerreiro, P. S.; Jose, R. *DNA Repair and Resistance to Cancer Therapy*; IntechOpen, 2013.

(8) Gavande, N. S.; VanderVere-Carozza, P. S.; Hinshaw, H. D.; Jalal, S. I.; Sears, C. R.; Pawelczak, K. S.; Turchi, J. J. DNA repair targeted therapy: the past or future of cancer treatment? *Pharmacol. Ther.* **2016**, *160*, 65−83.

(9) Roos, W. P.; Frohnapfel, L.; Quiros, S.; Ringel, F.; Kaina, B. XRCC3 contributes to temozolomide resistance of glioblastoma cells by promoting DNA double-strand break repair. *Cancer Lett.* **2018**, *424*, 119−126.

(10) Hansen, L. T.; Lundin, C.; Helleday, T.; Poulsen, H. S.; Sørensen, C. S.; Petersen, L. N.; Spang-Thomsen, M. DNA repair rate and etoposide (VP-16) resistance of tumor cell subpopulations derived from a single human small cell lung cancer. *Lung Cancer* **2003**, *40*, 157−164.

(11) Hou, W.-H.; Chen, S.-H.; Yu, X. Poly-ADP ribosylation in DNA damage response and cancer therapy. *Mutat. Res.* **2019**, *780*, 82−91.

(12) Lord, C. J.; Ashworth, A. PARP inhibitors: Synthetic lethality in the clinic. *Science* **2017**, *355*, 1152−1158.

(13) D'Andrea, A. D. Mechanisms of PARP inhibitor sensitivity and resistance. *DNA Repair* **2018**, *71*, 172−176.

(14) Pratz, K. W.; Rudek, M. A.; Gojo, I.; Litzow, M. R.; Mcdevitt, M. A.; Ji, J.; Karnitz, L. M.; Herman, J. G.; Kinders, R. J.; Smith, B. D.; Gore, S. D.; Carraway, H. E.; Showel, M. M.; Gladstone, D. E.; Levis, M. J.; Tsai, H.-L.; Rosner, G.; Chen, A.; Kaufmann, S. H.; Karp, J. E. A Phase I Study of Topotecan, Carboplatin and the PARP Inhibitor Veliparib in Acute Leukemias, Aggressive Myeloproliferative Neoplasms, and Chronic Myelomonocytic Leukemia. *Clin. Cancer Res.* **2017**, *23*, 899−907.

(15) Wahner Hendrickson, A. E.; Menefee, M. E.; Hartmann, L. C.; Long, H. J.; Northfelt, D. W.; Reid, J. M.; Boakye-Agyeman, F.; Kayode, O.; Flatten, K. S.; Harrell, M. I.; Swisher, E. M.; Poirer, G. G.; Satele, D.; Allred, J.; Lensing, J. L.; Chen, A.; Ji, J.; Zang, Y.; Erlichman, C.; Haluska, P.; Kaufmann, S. H. A Phase I Clinical Trial of the Poly(ADP-ribose) Polymerase Inhibitor Veliparib and Weekly Topotecan in Patients with Solid Tumors. *Clin. Cancer Res.* **2018**, *24*, 744−752.

(16) Ruscetti, T.; Lehnert, B. E.; Halbrook, J.; Le Trong, H.; Hoekstra, M. F.; Chen, D. J.; Peterson, S. R. Stimulation of the DNA-dependent Protein Kinase by Poly(ADP-Ribose) Polymerase. *J. Biol. Chem.* **1998**, *273*, 14461−14467.

(17) Ariumi, Y.; Masutani, M.; Copeland, T. D.; Mimori, T.; Sugimura, T.; Shimotohno, K.; Ueda, K.; Hatanaka, M.; Noda, M. Suppression of the poly(ADP-ribose) polymerase activity by DNA-dependent protein kinase in vitro. *Oncogene* **1999**, *18*, 4616−4625.

(18) Veuger, S. J.; Curtin, N. J.; Richardson, C. J.; Smith, G.C. M.; Durkacz, B. W. Radiosensitization and DNA Repair Inhibition by the Combined Use of Novel Inhibitors of DNA-dependent Protein Kinase

and Poly(ADP-Ribose) Polymerase-1. *Cancer Res.* **2003**, *63*, 6008−6015.

(19) Watanabe, G.; Lieber, M.; Williams, D. Structural step forward for NHEJ. *Cell Res.* **2017**, *27*, 1304−1306.

(20) Beskow, C.; Skikuniene, J.; Holgersson, Å.; Nilsson, B.; Lewensohn, R.; Kanter, L.; Viktorsson, K. Radioresistant cervical cancer shows upregulation of the NHEJ proteins DNA-PKcs, Ku70 and Ku86. *Br. J. Cancer* **2009**, *101*, 816−821.

(21) Bouchaert, P.; Guerif, S.; Debiais, C.; Irani, J.; Fromont, G. DNA-PKcs expression predicts response to radiotherapy in prostate cancer. *Int. J. Radiat. Oncol., Biol., Phys.* **2012**, *84*, 1179−1185.

(22) Lu, J.; Tang, M.; Li, H.; Xu, Z.; Weng, X.; Li, J.; Yu, X.; Zhao, L.; Liu, H.; Hu, Y.; Tan, Z.; Yang, L.; Zhong, M.; Zhou, J.; Fan, J.; Bode, A. M.; Yi, W.; Gao, J.; Sun, L.; Cao, Y. EBV-LMP1 suppresses the DNA damage response through DNA-PK/AMPK signaling to promote radioresistance in nasopharyngeal carcinoma. *Cancer Lett.* **2016**, *380*, 191−200.

(23) Li, D.; Luo, Y.; Chen, X.; Zhang, L.; Wang, T.; Zhuang, Y.; Fan, Y.; Xu, J.; Chen, Y.; Wu, L. NF-κB and poly (ADP-ribose) polymerase 1 form a positive-feedback loop that regulates DNA repair in acute myeloid leukemia cells. *Mol. Cancer Res.* **2019**, *17*, 761−772.

(24) Neal, J. A.; Seiji, S. M.; Carozza, PV.; Wagner, M.; Turchi, J.; Lees-Miller, S. P. Unraveling the Complexities of DNA-Dependent Protein Kinase Autophosphorylation. *MCB* **2014**, *34*, 2162−2175.

(25) Li, L. P.; Wu, X. D.; Sun, Y. X.; Chen, L. J. Establishing NHEJ repair quantitative detection system and detecting the roles of topoisomerase inhibitors etoposide VP-16 on NHEJ. *J. Med. Res.* **2015**, *4*, 26−30.

(26) Chang, H. H. Y.; Pannunzio, N. R.; Adachi, N.; Lieber, M. R. Non-homologous DNA end joining and alternative pathways to double-strand break repair. *Nat. Rev. Mol. Cell Biol.* **2017**, *18*, 495−506.

(27) Han, Y.; Jin, F.; Xie, Y.; Liu, Y.; Hu, S.; Liu, X. D.; Guan, H.; Gu, Y. Q.; MA, T.; Zhou, P. K. DNA-PKcs PARylation regulates DNA-PK kinase activity in the DNA damage response. *Mol. Med. Rep.* **2019**, *20*, 3609−3616.

(28) Douglas, P.; Cui, X.; Block, W. D.; Yu, Y.; Gupta, S.; Ding, Q.; Ye, R.; Morrice, N.; Lees-Miller, S. P.; Meek, K. The DNA-dependent protein kinase catalytic subunit is phosphorylated in vivo on threonine 3950, a highly conserved amino acid in the protein kinase domain. *Mol. Cell. Biol.* **2007**, *27*, 1581−1591.

(29) Lord, C. J.; Ashworth, A. The DNA damage response and cancer therapy. *Nature* **2012**, *481*, 287−294.

(30) Zhao, Y.; Thomas, H. D.; Batey, M. A.; Cowell, I. G.; Richardson, C. J.; Griffin, R. J.; Calvert, A. H.; Newell, D. R.; Smith, G. C. M.; Curtin, N. J. Preclinical Evaluation of a Potent Novel DNA-Dependent Protein Kinase Inhibitor NU7441. *Cancer Res.* **2006**, *66*, 5354−5362.

(31) Gunderson, C. C.; Moore, K. N. Olaparib: an oral PARP-1 and PARP-2 inhibitor with promising activity in ovarian cancer. *Future Oncol.* **2015**, *11*, 747−757.

(32) Min, A.; Im, S.-A.; Yoon, Y.-K.; Song, S.-H.; Nam, H.-J.; Hur, H.-S.; Kim, H.-P.; Lee, K.-H.; Han, S.-W.; Oh, D.-Y.; Kim, T.-Y.; O'Connor, M. J.; Kim, W.-H.; Bang, Y.-J. RAD51C-Deficient cancer cells are highly sensitive to the PARP inhibitor Olaparib. *Mol. Cancer Ther.* **2013**, *12*, 865−877.

(33) Kötter, A.; Cornils, K.; Borgmann, K.; et al. Inhibition of PARP1-dependent end-joining contributes to Olaparib-mediated radiosensitization in tumor cells. *Mol. Oncol.* **2014**, *8*, 1616−1625.

(34) Stover, E. H.; Konstantinopoulos, P. A.; Matulonis, U. A.; Swisher, E. M. Biomarkers of Response and Resistance to DNA Repair Targeted Therapies. *Clin. Cancer Res.* **2016**, *22*, 5651.

(35) Patel, A. G.; Sarkaria, J. N.; Kaufmann, S. H.; Anand, G.; Jann, N.; Sarkaria. Nonhomologous end joining drives poly(ADP-ribose)-polymerase (PARP) inhibitor lethality in homologous recombination-deficient cells. *Proc. Natl. Acad. Sci. U.S.A.* **2011**, *108*, 3406−3411.

(36) Wang, X.; Weaver, D. T. The ups and downs of DNA repair biomarkers for PARP inhibitor therapies. *Am. J. Cancer Res.* **2011**, *1*, 301−327.

(37) Morrison, C.; Smith, G. C. M.; Stingl, L.; Jackson, S. P.; Wagner, E. F.; Wang, Z.-Q. Genetic interaction between PARP and DNA-PK in

V(D)J recombination and tumorigenesis. *Nat. Genet.* **1997**, *17*, 479−482.

(38) Henrie, M. S.; Kurimasa, A.; Burma, S.; Ménissier-de Murcia, J.; de Murcia, G.; Li, G. C.; Chen, D. J. Lethality in PARP-1/Ku80 double mutant mice reveals physiological synergy during early embryogenesis. *DNA Repair* **2003**, *2*, 151−158.

(39) Galande, S.; Kohwi-Shigematsu, T. Poly(ADP-ribose) polymerase and Ku autoantigen form a complex and synergistically bind to matrix attachment sequences. *J. Biol. Chem.* **1999**, *274*, 20521−20528.

(40) Hossain, M. B.; Ji, P.; Anish, R.; Jacobson, R. H.; Takada, S. Poly(ADP-ribose) polymerase 1 interacts with nuclear respiratory factor 1 (NRF-1) and plays a role in NRF-1transcriptional regulation. *J. Biol. Chem.* **2009**, *284*, 8621−8632.

(41) Mitchell, J.; Smith, G. C. M.; Curtin, N. J. Poly(ADP-Ribose)polymerase-1 and DNA-dependent protein kinase have equivalent roles in double strand break repair following ionizing radiation. *Int. J. Radiat. Oncol., Biol., Phys.* **2009**, *75*, 1520−1527.

(42) Wang, H.; Perrault, A. R.; Takeda, Y.; Qin, W.; Iliakis. Biochemical evidence for Ku-independent backup pathways of NHEJ. *Nucleic Acids Res.* **2003**, *31*, 5377−5388.

(43) Spagnolo, L.; Barbeau, J.; Curtin, N. J.; Morris, E. P.; Pearl, L. H. Visualization of a DNA-PK/PARP1 complex. *Nucleic Acids Res.* **2012**, *40*, 4168−4177.

(44) Fok, J. H. L.; Ramos-Montoya, A.; Vazquez-Chantada, M.; Wijnhoven, P. W. G.; Follia, V.; James, N.; Farrington, P. M.; Karmokar, A.; Willis, S. E.; Cairns, J.; Nikkilä, J.; Beattie, D.; Lamont, G. M.; Finlay, M. R. V.; Wilson, J.; Smith, A.; O'Connor, L. O.; Ling, S.; Fawell, S. E.; O'Connor, M. J.; Hollingsworth, S. J.; Dean, E.; Goldberg, F. W.; Davies, B. R.; Cadogan, E. B. AZD7648 is a potent and selective DNA-PK inhibitor that enhances radiation, chemotherapy and olaparib activity. *Nat. Commun.* **2019**, *10*, 5065−5070.

(45) Zeng, L.; Boggs, D. H.; Xing, C.; Zhang, Z.; Anderson, J. C.; Wajapeyee, N.; Veale, C.; Bredel, M.; Shi, L. Z.; Bonner, J. A.; Willey, C. D.; Yang, E. S. Combining PARP and DNA-PK Inhibitors With Irradiation Inhibits HPV-Negative Head and Neck Cancer Squamous Carcinoma Growth. *Front. Genet.* **2020**, *11*, 1036.

(46) Cheema, T. A.; Kanai, R.; Kim, G. W.; Wakimoto, H.; Passer, B.; Rabkin, S. D.; Martuza, R. L. Enhanced antitumor efficacy of low-dose Etoposide with oncolytic herpes simplex virus in human glioblastoma stem cell xenografts. *Clin. Cancer Res.* **2011**, *17*, 7383−7393.